

# COMPUTER-AIDED DIAGNOSIS FOR PROSTATE CANCER USING MP-MRI

PhD Defence  
28<sup>th</sup> November 2016

Guillaume Lemaître

*Universitat de Girona - ViCOROB  
Université de Bourgogne Franche-Comté - LE2I*

Supervised by:

Robert Martí - Fabrice Mériadeau  
Jordi Freixenet - Paul M. Walker



- 1** Introduction
- 2** State-of-the-art
- 3** I2CVB
- 4** Toward a mp-MRI CAD for CaP
- 5** Experiments
- 6** Conclusions

## 1 Introduction

Motivations

The prostate organ

Prostate carcinoma

Screening

CAD and mp-MRI

Research objectives

## 2 State-of-the-art

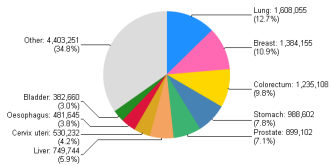
## 3 I2CVB

## 4 Toward a mp-MRI CAD for CaP

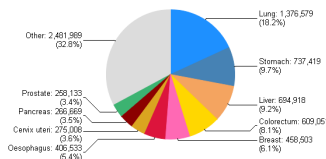
## 5 Experiments

## 6 Conclusions

## Statistics



(a) # of cancer cases



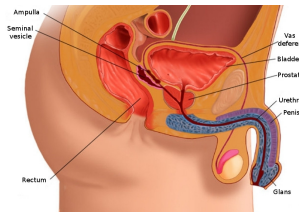
(b) # of cancer deaths

## Implications<sup>1</sup>

- ▶ 2<sup>nd</sup> most frequently diagnosed men cancer
  - ▶ Accounting for 7.1% of overall cancers diagnosed
  - ▶ Accounting for 3.4% of overall cancers death

<sup>1</sup> J. Ferlay et al. "Estimates of worldwide burden of cancer in 2008: GLOBOCAN 2008". In: *Int. J. Cancer* 127.12 (Dec. 2010), pp. 2893–2917.

Anatomy



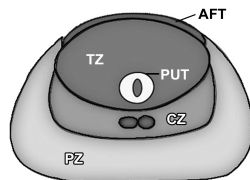
Localization of the prostate organ, image source<sup>2</sup>

## Characteristics

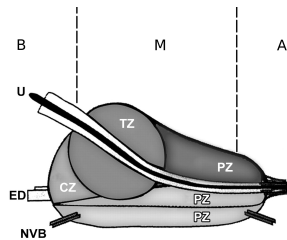
- ▶ Height: 3 cm
  - ▶ Depth: 2.5 cm
  - ▶ Weight: 7g to 16g

<sup>2</sup> **Geckomedia.** *Natom Anatomy.* French. June 2011. URL: <http://www.natomshop.com/>.

Anatomy



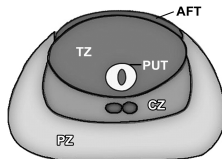
(a) Transverse plane



(b) Sagittal plane

Prostate zones - AFT: anterior fibromuscular tissue, CZ: central zone, ED: ejaculatory duct, NVB: neurovascular bundle, PUT: periurethral tissue, PZ: peripheral zone, U: urethra, TZ: transitional zone, B: base, M: median, A: apex; image source<sup>3</sup>

<sup>3</sup>Y. J. Choi et al. "Functional MR imaging of prostate cancer". In: *Radiographics* 27 (2007), pp. 63-75.



CaP development

- ▶ Slow-growing → 85 %
  - ▶ Fast-growing → 15 %
  - ▶ CaPs in CG are more aggressive

## Zonal predisposition

- ▶ PZ → 70 % to 80 %
  - ▶ TZ → 10 % to 20 %
  - ▶ CG → 5 %

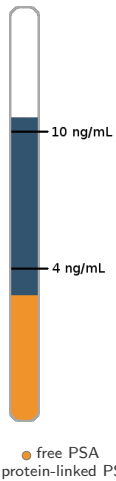
## Goals

- ▶ Detect CaP
  - ▶ Distinguish slow- from fast-growing CaP
  - ▶ Active surveillance vs. prostatectomy/other treatments

## Prostate-specific antigen

- ▶  $> 10 \text{ ng mL}^{-1} \rightarrow \text{biopsy}$
  - ▶ From  $4 \text{ ng mL}^{-1}$  to  $10 \text{ ng mL}^{-1}$   
 $\rightarrow \frac{\text{●}}{\text{○} + \text{●} + \text{○}} > 15\% \rightarrow \text{biopsy}$

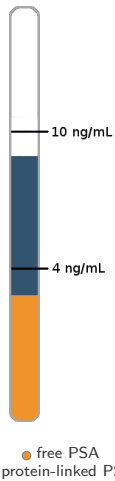
## “Blind” transrectal ultrasound biopsy



## Prostate-specific antigen

- ▶  $> 10 \text{ ng mL}^{-1} \rightarrow \text{biopsy}$
  - ▶ From  $4 \text{ ng mL}^{-1}$  to  $10 \text{ ng mL}^{-1}$   
 $\rightarrow \frac{\text{orange}}{\text{orange} + \text{blue}} > 15\% \rightarrow \text{biopsy}$

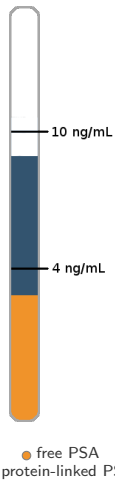
## “Blind” transrectal ultrasound biopsy



## Prostate-specific antigen

- ▶  $> 10 \text{ ng mL}^{-1} \rightarrow \text{biopsy}$
  - ▶ From  $4 \text{ ng mL}^{-1}$  to  $10 \text{ ng mL}^{-1}$   
 $\rightarrow \frac{\bullet}{\bullet + \circ} > 15\% \rightarrow \text{biopsy}$

## “Blind” transrectal ultrasound biopsy



## Prostate-specific antigen

- ▶  $> 10 \text{ ng mL}^{-1} \rightarrow \text{biopsy}$
  - ▶ From  $4 \text{ ng mL}^{-1}$  to  $10 \text{ ng mL}^{-1}$   
 $\rightarrow \frac{\text{orange}}{\text{orange} + \text{blue}} > 15\% \rightarrow \text{biopsy}$

## “Blind” transrectal ultrasound biopsy

- ▶ Take samples from different locations
  - ▶ Grade using Gleason score

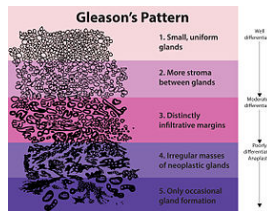


Image source: <https://goo.gl/fEVQXQ>

## Prostate-specific antigen

- ▶  $> 10 \text{ ng mL}^{-1} \rightarrow \text{biopsy}$
  - ▶ From  $4 \text{ ng mL}^{-1}$  to  $10 \text{ ng mL}^{-1}$   
 $\rightarrow \frac{\text{orange}}{\text{orange} + \text{blue}} > 15\% \rightarrow \text{biopsy}$

## “Blind” transrectal ultrasound biopsy

- ▶ Take samples from different locations
  - ▶ Grade using Gleason score

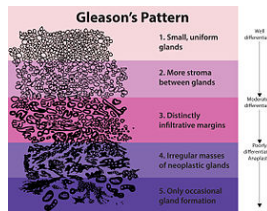


Image source: <https://goo.gl/fEVQXQ>

## Prostate-specific antigen

- ▶  $> 10 \text{ ng mL}^{-1} \rightarrow \text{biopsy}$
  - ▶ From  $4 \text{ ng mL}^{-1}$  to  $10 \text{ ng mL}^{-1}$   
 $\rightarrow \frac{\bullet}{\bullet + \bullet} > 15\% \rightarrow \text{biopsy}$

“Blind” transrectal ultrasound biopsy

- ▶ Take samples from different locations
  - ▶ Grade using Gleason score

## Pros

- ✓ Reduce CaP-related mortality from 21 % to 44 %<sup>4</sup>

Cons

- ✗ Up to 30 % of over-diagnosis<sup>5</sup>
  - ✗ Up to 35 % of undiagnosed CaP<sup>6</sup>
  - ✗ Biopsies are invasive

<sup>4</sup>Fritz H. Schröder et al. "Prostate-cancer mortality at 11 years of follow-up". In: *New England Journal of Medicine* 366.11 (2012), pp. 981-990.

<sup>5</sup> G. P. Haas et al. "Needle biopsies on autopsy prostates: sensitivity of cancer detection based on true prevalence". In: *J. Natl. Cancer Inst.* 99.19 (Oct. 2007), pp. 1484–1489.

<sup>6</sup> A. V. Taira et al. "Performance of transperineal template-guided mapping biopsy in detecting prostate cancer in the initial and repeat biopsy setting". In: *Prostate Cancer Prostatic Dis.* 13.1 (Mar. 2010), pp. 71-77.

## Pros

- ✓ Reduce CaP-related mortality from 21 % to 44 %<sup>7</sup>

## Cons

- ✗ Up to 30 % of over-diagnosis<sup>8</sup>
- ✗ Up to 35 % of undiagnosed CaP<sup>9</sup>
- ✗ Biopsies are invasive

<sup>7</sup>Schrder et al., "Prostate-cancer mortality at 11 years of follow-up".

<sup>8</sup>Haas et al., "Needle biopsies on autopsy prostates: sensitivity of cancer detection based on true prevalence".

<sup>9</sup>Taira et al., "Performance of transperineal template-guided mapping biopsy in detecting prostate cancer in the initial and repeat biopsy setting".

## Current trendy techniques: mp-MRI

- ✓ Less invasive technique

Human diagnosis using mp-MRI

- ✗ Need further investigation of the mp-MRI modalities
  - ✗ Low repeatability
    - ▶ Observer limitations
    - ▶ Complexity of clinical cases

## Emergence of CAD

- ▶ CADe → detection of potential lesions
  - ▶ CADx → diagnosis regarding those lesions

## Propose a mp-MRI CAD for CaP

- ▶ Study and investigate the state-of-the-art on MRI CAD for CaP
- ▶ Identify the scientific barriers
- ▶ Design a mp-MRI CAD addressing these issues
- ▶ Investigate and analyze the proposed CAD

1 Introduction

2 State-of-the-art

MRI modalities  
CAD for CaP

3 I2CVB

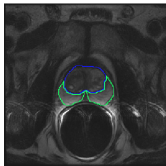
4 Toward a mp-MRI CAD for CaP

5 Experiments

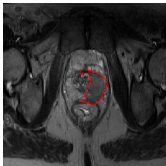
6 Conclusions

# MRI modalities

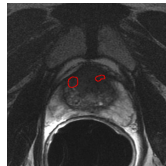
## T<sub>2</sub>W-MRI



(a) Healthy



(b) CaP PZ



(c) CaP CG

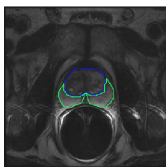
### Healthy

- ▶ Intermediate to high-signal intensity (SI) in PZ
- ▶ Low-SI in CG

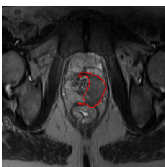
### CaP

- ▶ Low-SI
- ▶ Round and ill-defined mass in PZ
- ▶ Homogeneous with ill-defined edges in CG

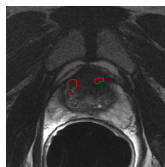
## T<sub>2</sub>W-MRI



(d) Healthy



(e) CaP PZ



(f) CaP CG

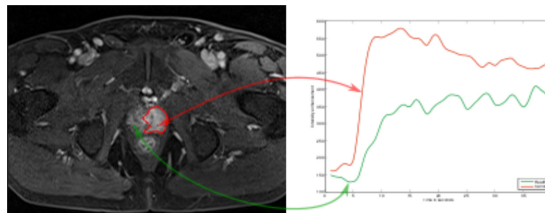
### Pros

- ▶ Highest spatial resolution
- ▶ Anatomy nicely depicted

### Cons

- ▶ Low sensitivity in CG
- ▶ Lower specificity due to outliers

DCE-MRI



**Green:** healthy - **Red:** CaP

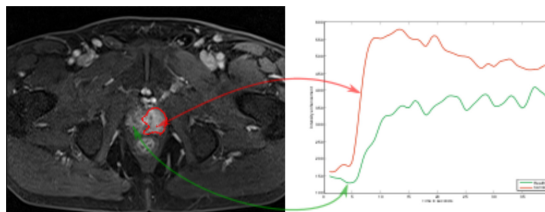
## Healthy

- ▶ Slower wash-in, wash-out, time-to-peak enhancement
  - ▶ Lower integral under the curve, max SI

CaP

- ▶ Faster wash-in, wash-out, time-to-peak enhancement
  - ▶ Higher integral under the curve, max SI

## DCE-MRI



Green: healthy - Red: CaP

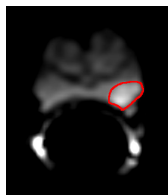
## Pros

- ▶ Information about vascularity

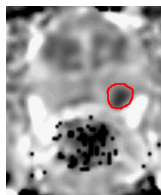
## Cons

- ▶ Spatial mis-registration
- ▶ Lower spatial resolution than  $T_2$ W-MRI
- ▶ Difficult detection in CG

## DW-MRI - ADC



(a) DW MRI



(b) ADC

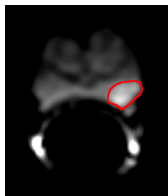
## Healthy

- ▶ DW-MRI: lower SI
- ▶ ADC: higher-SI

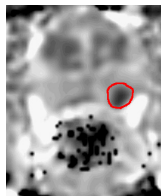
## CaP

- ▶ DW-MRI: higher SI
- ▶ ADC: lower-SI

## DW-MRI - ADC



(c) DW MRI



(d) ADC

## Pros

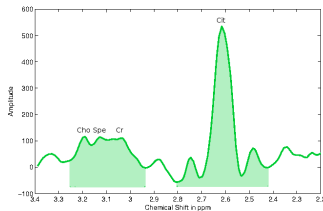
- ▶ Information about tissue structure
- ▶ ADC correlated with Gleason score

## Cons

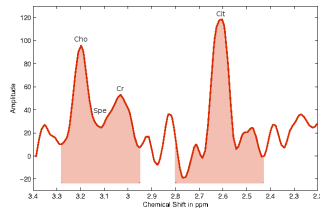
- ▶ Poor spatial resolution
- ▶ Variability of the ADC coefficient

# MRI modalities

## MRSI



(a) Healthy



(b) CaP

### Healthy

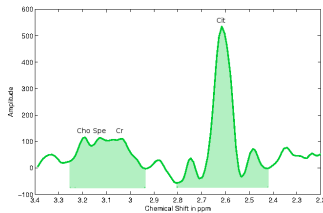
- ▶ High citrate
- ▶ Moderate choline and spermine

### CaP

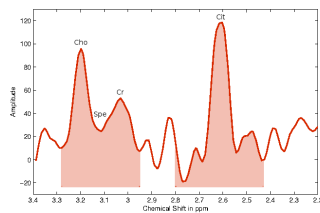
- ▶ Decrease of citrate and spermine
- ▶ Increase of choline

# MRI modalities

## MRSI



(c) Healthy



(d) CaP

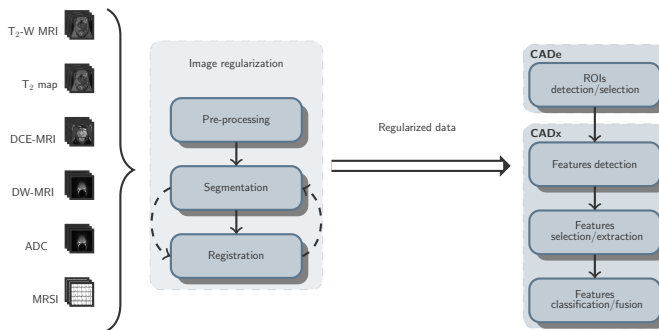
### Pros

- Citrate correlated with Gleason score

### Cons

- Low spatial resolution
- Variation inter-patients

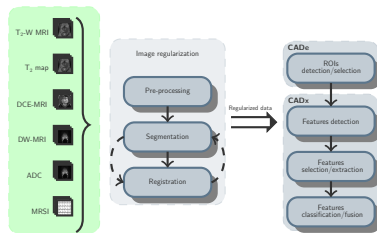
## Full CAD for detection and diagnosis of CaP



Common CAD framework based on MRI images used to detect CaP

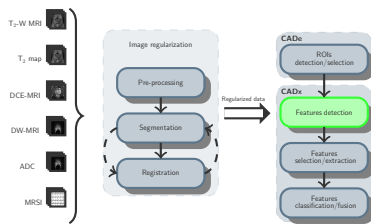
## Conclusions

- ✓ 3 modalities better than 2
- ✓ Texture and edge features are predominant
- ✓ Features selection/extraction tends to improve performance
- ✓ Pre-eminence of SVM and ensemble classifier (i.e., AdaBoost, RF, etc.)



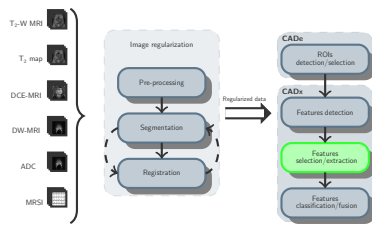
## Conclusions

- ✓ 3 modalities better than 2
- ✓ Texture and edge features are predominant
- ✓ Features selection/extraction tends to improve performance
- ✓ Pre-eminence of SVM and ensemble classifier (i.e., AdaBoost, RF, etc.)



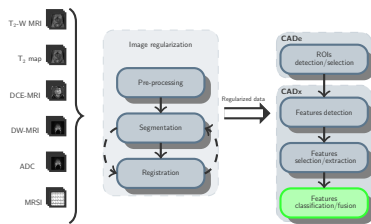
## Conclusions

- ✓ 3 modalities better than 2
- ✓ Texture and edge features are predominant
- ✓ Features selection/extraction tends to improve performance
- ✓ Pre-eminence of SVM and ensemble classifier (i.e., AdaBoost, RF, etc.)



## Conclusions

- ✓ 3 modalities better than 2
- ✓ Texture and edge features are predominant
- ✓ Features selection/extraction tends to improve performance
- ✓ Pre-eminence of SVM and ensemble classifier (i.e., AdaBoost, RF, etc.)





# CAD for CaP

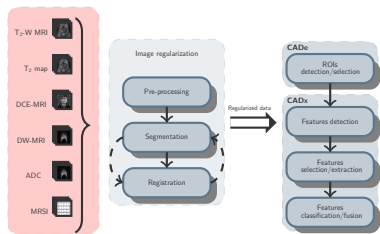


## Conclusions

- ✓ 3 modalities better than 2
- ✓ Texture and edge features are predominant
- ✓ Features selection/extraction tends to improve performance
- ✓ Pre-eminence of SVM and ensemble classifier (i.e., AdaBoost, RF, etc.)

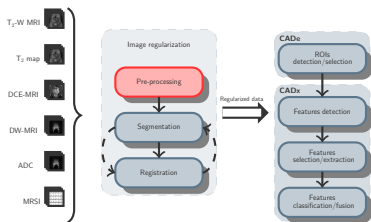
## Scientific and technical challenges

- ✗ No publicly available mp-MRI dataset
- ✗ Only 1 study used 4 MRI modalities
- ✗ Limited work on data normalization
- ✗ A lot of features are extracted in 2D
- ✗ Limited work regarding selection/extraction
- ✗ No work regarding data balancing
- ✗ No source code available of any CAD



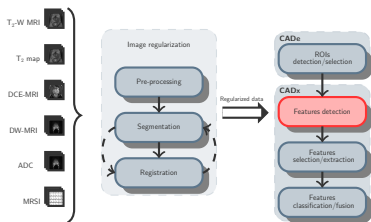
## Scientific and technical challenges

- ✗ No publicly available mp-MRI dataset
- ✗ Only 1 study used 4 MRI modalities
- ✗ Limited work on data normalization
- ✗ A lot of features are extracted in 2D
- ✗ Limited work regarding selection/extraction
- ✗ No work regarding data balancing
- ✗ No source code available of any CAD



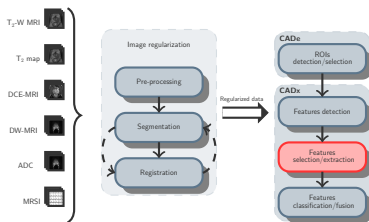
## Scientific and technical challenges

- ✗ No publicly available mp-MRI dataset
- ✗ Only 1 study used 4 MRI modalities
- ✗ Limited work on data normalization
- ✗ A lot of features are extracted in 2D
- ✗ Limited work regarding selection/extraction
- ✗ No work regarding data balancing
- ✗ No source code available of any CAD



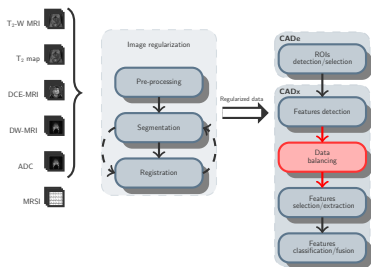
## Scientific and technical challenges

- ✗ No publicly available mp-MRI dataset
- ✗ Only 1 study used 4 MRI modalities
- ✗ Limited work on data normalization
- ✗ A lot of features are extracted in 2D
- ✗ Limited work regarding selection/extraction
- ✗ No work regarding data balancing
- ✗ No source code available of any CAD



## Scientific and technical challenges

- ✗ No publicly available mp-MRI dataset
- ✗ Only 1 study used 4 MRI modalities
- ✗ Limited work on data normalization
- ✗ A lot of features are extracted in 2D
- ✗ Limited work regarding selection/extraction
- ✗ No work regarding data balancing
- ✗ No source code available of any CAD



## Scientific and technical challenges

- ✗ No publicly available mp-MRI dataset
- ✗ Only 1 study used 4 MRI modalities
- ✗ Limited work on data normalization
- ✗ A lot of features are extracted in 2D
- ✗ Limited work regarding selection/extraction
- ✗ No work regarding data balancing
- ✗ No source code available of any CAD

## Conclusions

- ✓ 3 modalities better than 2
- ✓ Texture and edge features are predominant
- ✓ Features selection/extraction tends to improve performance
- ✓ Pre-eminence of SVM and ensemble classifier (i.e., AdaBoost, RF, etc.)

## Scientific and technical challenges

- ✗ No publicly available mp-MRI dataset
- ✗ Only 1 study used 4 MRI modalities
- ✗ Limited work on data normalization
- ✗ A lot of features are extracted in 2D
- ✗ Limited work regarding selection/extraction
- ✗ No work regarding data balancing
- ✗ No source code available of any CAD

## Conclusions

- ✓ 3 modalities better than 2
- ✓ Texture and edge features are predominant
- ✓ Features selection/extraction tends to improve performance
- ✓ Pre-eminence of SVM and ensemble classifier (i.e., AdaBoost, RF, etc.)

## Scientific and technical challenges

- ✗ No publicly available mp-MRI dataset
- ✗ Only 1 study used 4 MRI modalities
- ✗ Limited work on data normalization
- ✗ A lot of features are extracted in 2D
- ✗ Limited work regarding selection/extraction
- ✗ No work regarding data balancing
- ✗ No source code available of any CAD

## Research objectives

- ▶ Collect a mp-MRI dataset
- ▶ Design a CAD for CaP using all mp-MRI modalities
- ▶ Investigate normalization, feature selection/extraction, data balancing
- ▶ Implement 3D features
- ▶ Release source code and dataset

## 1 Introduction

## 2 State-of-the-art

## 3 I2CVB

Mp-MRI prostate datasets

Open source initiative

I2CVB

## 4 Toward a mp-MRI CAD for CaP

## 5 Experiments

## 6 Conclusions



## 1.5 T General Electric scanner

- ▶ T<sub>2</sub>W-MRI, DW-MRI, DCE-MRI, and MRSI
- ▶ Ground-truth (GT) for CaP, PZ, and CG associated to T<sub>2</sub>W-MRI modality
- ▶ Healthy: 4 vs. CaP: { PZ: 14 + 3, CG: 0 + 3 }

## 3 T Siemens scanner

- ▶ T<sub>2</sub>W-MRI, ADC, DCE-MRI, and MRSI
- ▶ GT for CaP, PZ, and CG associated to T<sub>2</sub>W-MRI modality
- ▶ Additional GT of the prostate for DCE-MRI and ADC
- ▶ Healthy: 2 vs. CaP: { PZ: 12 + 2, CG: 3 + 2 }



## 1.5 T General Electric scanner

- ▶ T<sub>2</sub>W-MRI, DW-MRI, DCE-MRI, and MRSI
- ▶ Ground-truth (GT) for CaP, PZ, and CG associated to T<sub>2</sub>W-MRI modality
- ▶ Healthy: 4 vs. CaP: { PZ: 14 + 3, CG: 0 + 3 }

## 3 T Siemens scanner

- ▶ T<sub>2</sub>W-MRI, ADC, DCE-MRI, and MRSI
- ▶ GT for CaP, PZ, and CG associated to T<sub>2</sub>W-MRI modality
- ▶ Additional GT of the prostate for DCE-MRI and ADC
- ▶ Healthy: 2 vs. CaP: { PZ: 12 + 2, CG: 3 + 2 }



# Open source initiative



## protoclass toolbox

- ▶ Data management
- ▶ Features detection

## imbalanced-learn toolbox<sup>10</sup>

- ▶ Part of the scikit-learn-contrib projects

## Third-party toolboxes



<sup>10</sup> Guillaume Lemaitre et al. "Imbalanced-learn: A Python Toolbox to Tackle the Curse of Imbalanced Datasets in Machine Learning". In: *Journal of Machine Learning Research* (2017).



# A web platform



## I<sub>2</sub>CVB platform

Initiative for Collaborative Computer Vision Benchmarking

Home Benchmarks Contact

ICCVB in a nutshell

I<sub>2</sub>CVB Vision

Tweets

I2CVB @I2CVB Just setting up my #myfirstTweet

Load More

## Hub for our different resources

- ▶ GitHub for our source codes
- ▶ Zenodo for our datasets
- ▶ HAL, arXiv, ResearchGate for our publications

1 Introduction

2 State-of-the-art

3 I2CVB

4 Toward a mp-MRI CAD for CaP

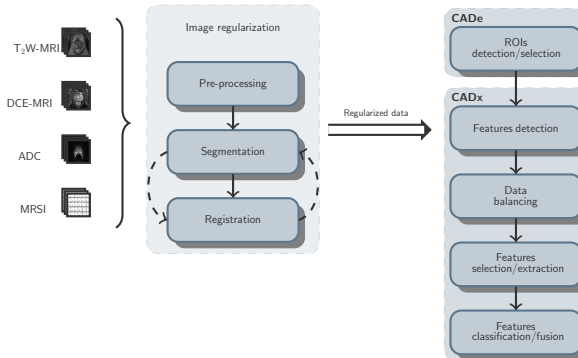
Image regularization

CADe-CADx

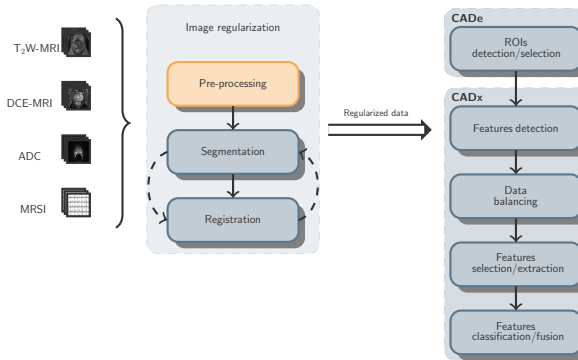
5 Experiments

6 Conclusions

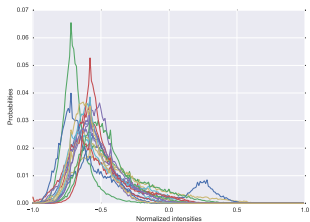
## Mp-MRI CAD for CaP



## Pre-processing

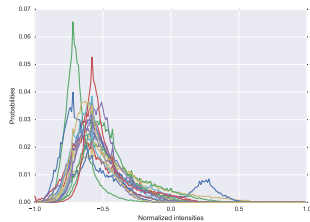


## Inter-patients intensity variations



- ▶ Artan et al.<sup>11</sup> and Ozer et al.<sup>12</sup> normalized data based on the *z-score*.
- ▶ Lv et al.<sup>13</sup> and Viswanath et al.<sup>14</sup> used methods based on piecewise-linear normalization<sup>15</sup>.

## Inter-patients intensity variations

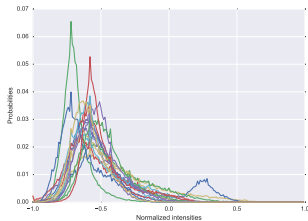


- ▶ Artan et al.<sup>11</sup> and Ozer et al.<sup>12</sup> normalized data based on the *z-score*.
- ▶ Lv et al.<sup>13</sup> and Viswanath et al.<sup>14</sup> used methods based on piecewise-linear normalization<sup>15</sup>.

<sup>11</sup> Y. Artan et al. "Prostate cancer localization with multispectral MRI using cost-sensitive support vector machines and conditional random fields". In: *IEEE Trans Image Process* 19.9 (Sept. 2010), pp. 2444–2455.

<sup>12</sup> S. Ozer et al. "Supervised and unsupervised methods for prostate cancer segmentation with multispectral MRI". In: *Med Phys* 37.4 (Apr. 2010), pp. 1873–1883.

## Inter-patients intensity variations



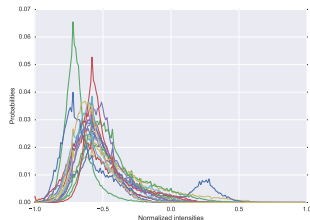
- ▶ Artan et al.<sup>11</sup> and Ozer et al.<sup>12</sup> normalized data based on the  $z$ -score.
- ▶ Lv et al.<sup>13</sup> and Viswanath et al.<sup>14</sup> used methods based on piecewise-linear normalization<sup>15</sup>.

<sup>13</sup>D. Lv et al. "Computerized characterization of prostate cancer by fractal analysis in MR images". In: *J Magn Reson Imaging* 30.1 (July 2009), pp. 161–168.

<sup>14</sup>S. E. Viswanath et al. "Central gland and peripheral zone prostate tumors have significantly different quantitative imaging signatures on 3 Tesla endorectal, in vivo T2-weighted MR imagery". In: *J Magn Reson Imaging* 36.1 (July 2012), pp. 213–224.

<sup>15</sup>L. G. Nyul et al. "New variants of a method of MRI scale standardization". In: *IEEE Trans Med Imaging* 19.2 (Feb. 2000), pp. 143–150.

## Inter-patients intensity variations



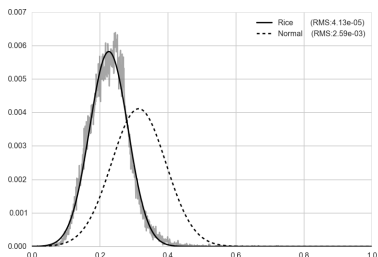
- ▶ Artan et al.<sup>11</sup> and Ozer et al.<sup>12</sup> normalized data based on the *z-score*.
- ▶ Lv et al.<sup>13</sup> and Viswanath et al.<sup>14</sup> used methods based on piecewise-linear normalization<sup>15</sup>.

## Contributions<sup>16</sup>

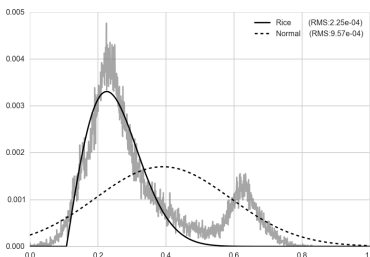
- (i) a *model-based* approach using Rician *a priori*
- (ii) a *non-parametric based* approach based on the SRSF representation

<sup>16</sup> Guillaume Lemaitre et al. "Normalization of T2W-MRI Prostate Images using Rician a priori". In: SPIE Medical Imaging. International Society for Optics and Photonics. 2016, pp. 978529–978529.

## Gaussian vs. Rician



(a) Patient #1



(b) Patient #2

Example of fitted functions



## Gaussian normalization

$$I_s(x) = \frac{I_r(x) - \mu_G}{\sigma_G} . \quad (1)$$

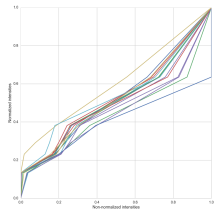
## Rician normalization

$$I_s(x) = \frac{I_r(x) - \mu_R}{\sigma_R} , \quad (2)$$

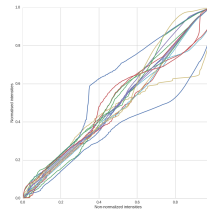
$$\mu_R = \sigma \sqrt{\frac{\pi}{2}} L_{1/2} \left( -\frac{\nu^2}{2\sigma^2} \right), \quad (3)$$

$$\sigma_R = 2\sigma^2 + \nu^2 - \frac{\pi\sigma^2}{2} L_{1/2}^2 \left( \frac{-\nu^2}{2\sigma^2} \right) . \quad (4)$$

## Comparison of warping function



(a) Piecewise-linear warping



(b) SRSF warping

## Piecewise-linear normalization

Minimize the distance between some standardized landmarks  $\mu_i$  and some non-normalized landmarks  $\lambda_i$

## SRSF-based normalization

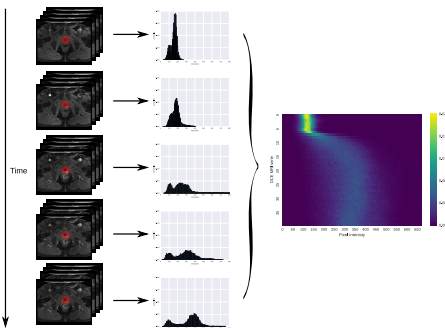
Minimize the distance between a mean PDF  $\mu_f$  (i.e., the Karcher mean) and a given patient PDF  $f_i$

# DCE-MRI normalization

## Contribution<sup>17</sup>

- ▶ Propose a method to normalize DCE-MRI data

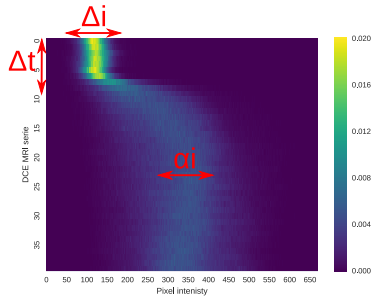
## Heatmap representation



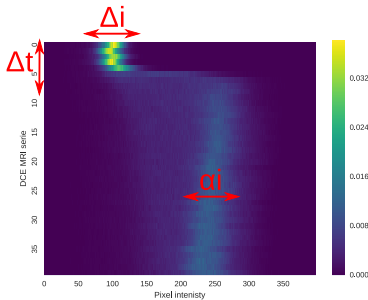
<sup>17</sup> Guillaume Lemaître et al. "Automatic prostate cancer detection through DCE-MRI images: all you need is a good normalization". In: *Medical Image Analysis - Submitted* (2017).

# DCE-MRI normalization

## Inter-patients variations



(a) Patient #1



(b) Patient #2

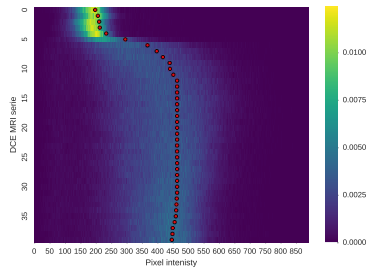
Variations driven by  $\Delta_i$ ,  $\Delta_t$ , and  $\sigma_i$

## DCE-MRI normalization

Correction of  $\Delta_i$ 

Find the shortest path in a directed weighted graph  $\mathcal{G} = (\mathcal{V}, \mathcal{E})$  with the edge weight  $w_{ij}$  between 2 nodes  $i$  and  $j$  corresponding to 2 pixels at position  $(x_i, y_i)$  and  $(x_j, y_j)$ , respectively defined as:

$$w_{ij} = \begin{cases} \alpha \exp(1 - \frac{H(i)}{\max(H)}) & \text{if } x_j = x_i + 1 \text{ and } y_j = y_i, \\ (1 - \alpha) \exp(1 - \frac{H(i)}{\max(H)}) & \text{if } x_j = x_i \text{ and } y_j = y_i + 1, \\ 0 & \text{otherwise,} \end{cases} \quad (5)$$



# DCE-MRI normalization

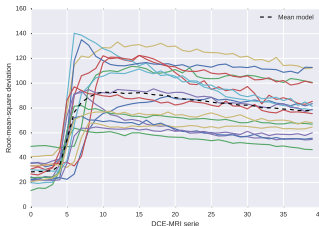
## Correction of $\Delta_t$ and $\sigma_i$

Register all RMSD to a mean model such that:

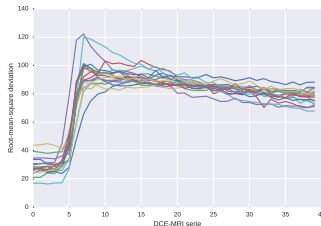
$$\arg \min_{\alpha, \tau} = \sum_{t=1}^N [T(\alpha, \tau, f(t)) - \mu(t)]^2, \quad (6)$$

$$f(t) = \sqrt{\left( \frac{\sum_{n=1}^N x(t)_n^2}{N} \right)}, \quad (7)$$

$$T(\alpha, \tau, f(t)) = \alpha f(t - \tau). \quad (8)$$



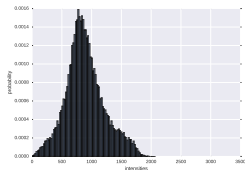
(a) RMSD before correction



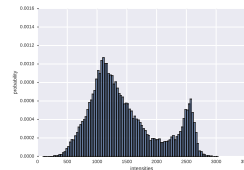
(b) Registered RMSD

## ADC normalization

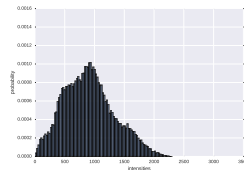
## Variability of PDF in ADC data



(a) Patient #1



(b) Patient #2

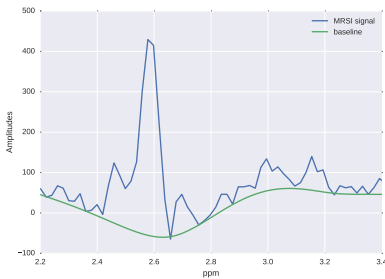


(c) Patient #3

- ▶ Piecewise-linear normalization

## MRSI pre-processing

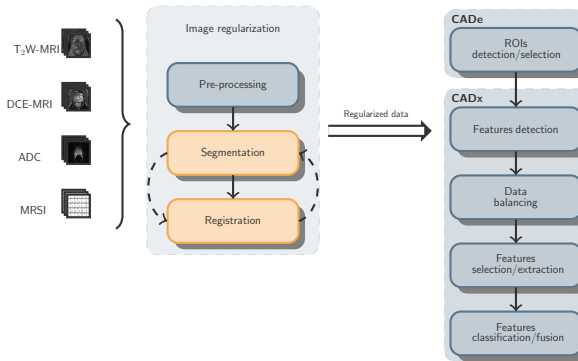
- ▶ Phase correction<sup>18</sup>
- ▶ Frequency alignment
- ▶ Baseline correction<sup>19</sup>



<sup>18</sup> Li Chen et al. "An efficient algorithm for automatic phase correction of {NMR} spectra based on entropy minimization ". In: *Journal of Magnetic Resonance* 158.12 (2002), pp. 164–168.

<sup>19</sup> Yuanxin Xi and David M Rocke. "Baseline correction for NMR spectroscopic metabolomics data analysis". In: *BMC bioinformatics* 9.1 (2008), p. 1.

## Segmentation & registration



## Interpolation

- ▶ ADC and DCE-MRI are interpolated to the T<sub>2</sub>W-MRI resolution

## Segmentation

- ▶ Manual prostate segmentation available for T<sub>2</sub>W-MRI, DCE-MRI, and ADC
- ▶ Cap, PZ, and CG manual segmentation available for T<sub>2</sub>W-MRI

## Registration

- ▶ Intra-patient motions correction in DCE-MRI: rigid registration using mutual information
- ▶ DCE-MRI is registered to T<sub>2</sub>W-MRI using the prostate segmentation
- ▶ ADC is registered to T<sub>2</sub>W-MRI using the prostate segmentation

## Features detection

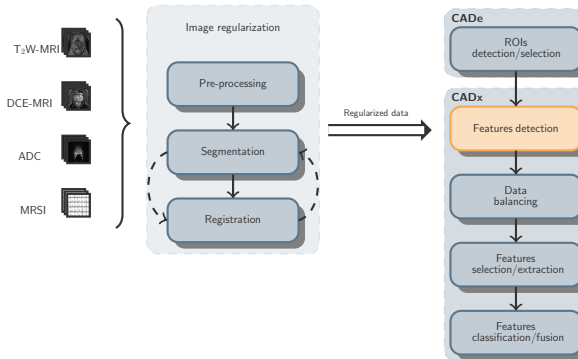


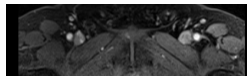
## Image features

Features	Parameters	# dimensions
Intensity		1
DCT decomposition	window: 9 px × 9 px × 3 px	243
Kirsch filter		2
Laplacian filter		1
Prewitt filter		3
Scharr filter		3
Sobel filter		3
Gabor filters	4 frequencies $f \in [0.05, 0.25]$ ; 4 azimuth angles $\alpha \in [0, \pi]$ ; 8 elevation angles $\alpha \in [0, 2\pi]$	256
Phase congruency filter	5 orientations; 6 scales	3
Haralick filter	window: 9 px × 9 px × 3 px; # grey levels: 8; distance: 1 px; 13 directions	169
LBP filter	2 radii $r = \{1, 2\}$ ; 2 neighborhood sizes $N = \{8, 16\}$	6

## Quantitative and semi-quantitative models

- ▶ Brix's model
- ▶ Hoffmann's model
- ▶ Tofts' model
- ▶ PUN model
- ▶ Semi-quantitative model
- ▶ Entire enhanced signal

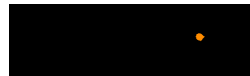
## Segmentation of arterial input function (AIF)



(a) Original



(b) Candidate

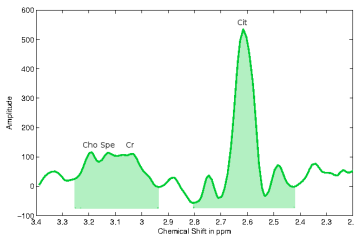


(c) AIF

- (i) K-means clustering with  $k = 6$
- (ii) Select the cluster with the highest 90<sup>th</sup> percentile
- (iii) Select regions with an eccentricity  $\mathcal{E} < 0.5$  and an area  $\mathcal{A} \in [100, 400]$

## Quantification strategies

- ▶ Quantification with fixed bounds
- ▶ Quantification by fitting some modeled signal
- ▶ Entire spectra

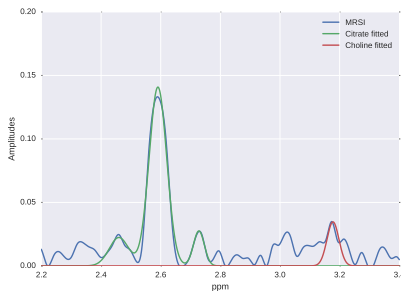


## Assumptions

- ▶ Integrate citrate from 2.46 ppm to 2.82 ppm
- ▶ Integrate choline from 3.19 ppm to 3.23 ppm

## Quantification strategies

- ▶ Quantification with fixed bounds
- ▶ Quantification by fitting some modeled signal
- ▶ Entire spectra



## Citrate quantification

$$\begin{aligned} \arg \min_{\mathbf{w}} \quad & |S(x) - M_1(x; \mathbf{w})|^2, \\ \text{subject to} \quad & 2.54 < \mu < 2.68, \\ & 0.06 < \delta_1, \delta_2 < 0.16, \\ & 0.01 < \sigma_1, \sigma_2, \sigma_3 < 0.1, \\ & \alpha_1, \alpha_2, \alpha_3 > 0. \end{aligned} \tag{9}$$

$$M_1(x; \mathbf{w}) = \alpha_1 \mathcal{N}(x; \mu, \sigma_1) + \alpha_2 \mathcal{N}(x; \mu + \delta_2, \sigma_2) + \alpha_3 \mathcal{N}(x; \mu - \delta_3, \sigma_3). \quad (10)$$

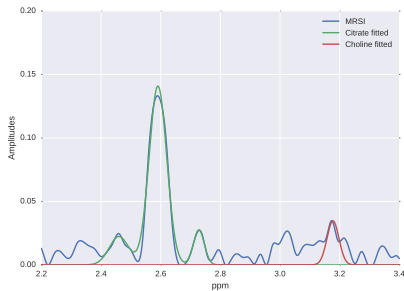
## Choline quantification

$$\begin{aligned} \arg \min_{\mu, \sigma} \quad & |S(x) - M_2(x; \mu, \sigma)|^2 , \\ \text{subject to} \quad & 3.17 < \mu < 3.21 , \\ & 0.001 < \sigma < 0.02 , \\ & \alpha > 0 . \end{aligned} \tag{11}$$

$$M_2(x; \mu, \sigma) = \alpha \mathcal{N}(x; \mu, \sigma) . \quad (12)$$

## Quantification strategies

- ▶ Quantification with fixed bounds
- ▶ Quantification by fitting some modeled signal
- ▶ Entire spectra



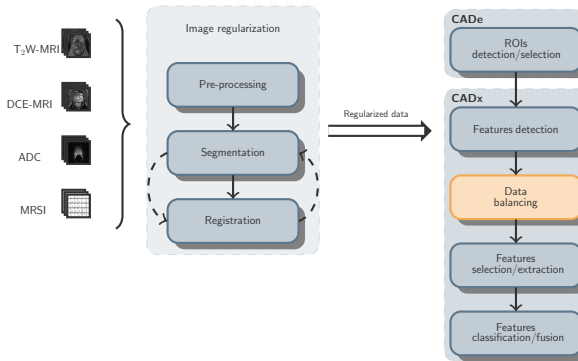
Metrics<sup>20, 21</sup>,

- ▶ Relative distance to the *prostate boundary*
- ▶ Relative distance to the *prostate center*
- ▶ Relative position in the *Euclidean* coordinate systems
- ▶ Relative position in the *cylindrical* coordinate systems

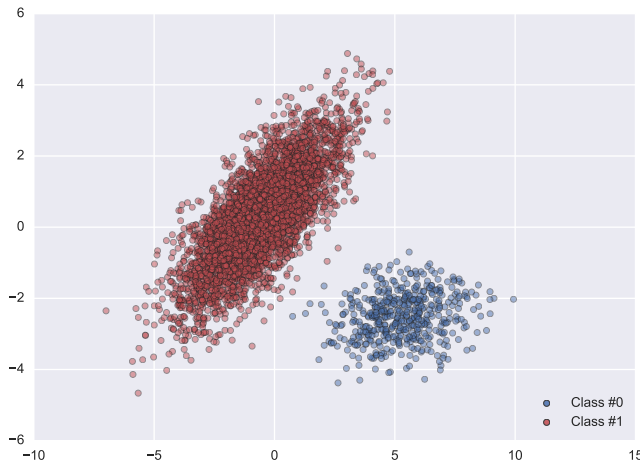
<sup>20</sup> Jeremy Chen et al. "Automatic determination of arterial input function for dynamic contrast enhanced MRI in tumor assessment". In: *International Conference on Medical Image Computing and Computer-Assisted Intervention*. Springer. 2008, pp. 594–601. doi: 10.1007/978-3-540-85988-8\_71.

<sup>21</sup> G. Litjens et al. "Computer-aided detection of prostate cancer in MRI". In: *Medical Imaging, IEEE Transactions on* 33.5 (May 2014), pp. 1083–1092. ISSN: 0278-0062.

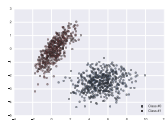
## Data balancing



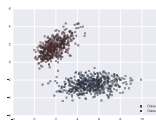
## Toy example



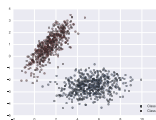
## Under-sampling



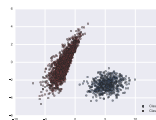
(a) NM1



(b) NM2

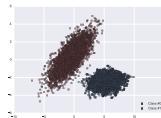


(c) NM3

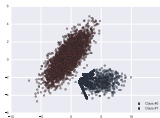


(d) NM3

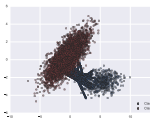
## Over-sampling



(e) SMOTE

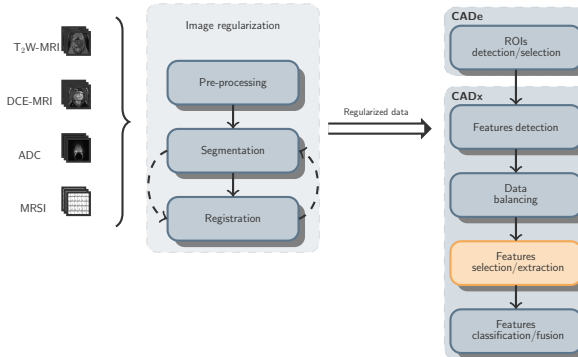


(f) SMOTE-b1



(g) SMOTE-b2

## Features selection/extraction



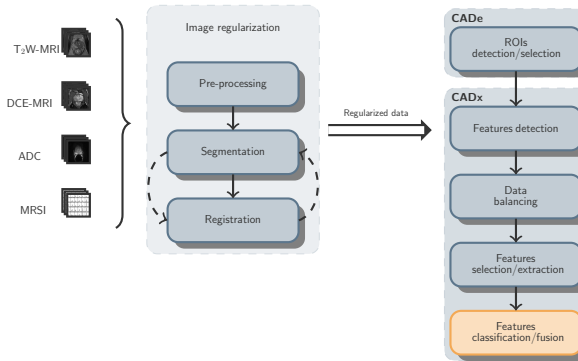
## Features extraction

- ▶ Independent components analysis (ICA)
- ▶ Principal components analysis (PCA)
- ▶ Sparse-PCA

## Features selection

- ▶ One-way analysis of variance (ANOVA)
- ▶ Gini importance

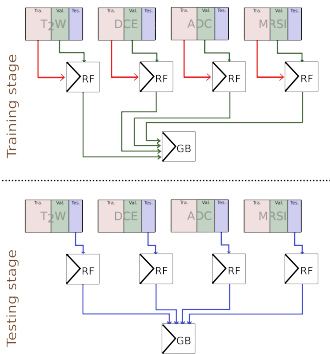
## Features classification



# Features classification

## Classifier

- ▶ Random forest (RF)
- ▶ Stacking of RF with an adaboost and gradient-boosting meta-classifier



## 1 Introduction

## 2 State-of-the-art

## 3 I2CVB

## 4 Toward a mp-MRI CAD for CaP

## 5 Experiments

T<sub>2</sub>W-MRI normalization

Standalone modalities

Coarse combination

Data balancing

Features selection/extraction

Fine-tuned combination

MRSI benefit

## 6 Conclusions



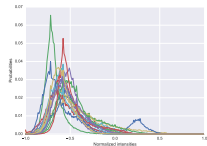
# T<sub>2</sub>W-MRI normalization<sup>22</sup>



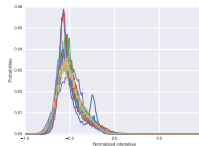
## Metric

- ▶ Variability of the mean intensity of a given tissue across patients
  - ✗ Statistically, the mean correspond a single point of the PDF
  - ✗ This point can be closely related to a landmark for the piecewise-linear normalization
- Make a PCA of the different PDFs
  - ✓ Comparison of the alignment of the entire PDF instead of a single point

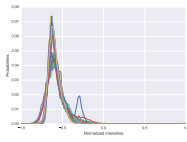
## Prostate data



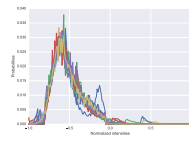
(a) Raw - AUC: 99.08



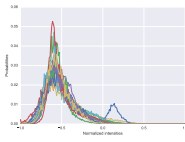
(b) Gaussian - AUC: 99.58



(c) Rician - AUC: 99.74

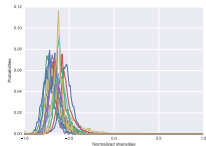


(d) Linear - AUC: 99.45

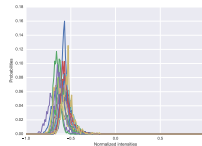


(e) SRSF - AUC: 99.12

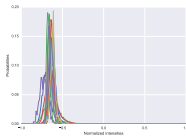
## CaP data



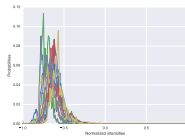
(a) Raw - AUC: 98.19



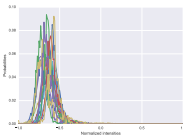
(b) Gaussian - AUC: 98.22



(c) Rician - AUC: 98.25

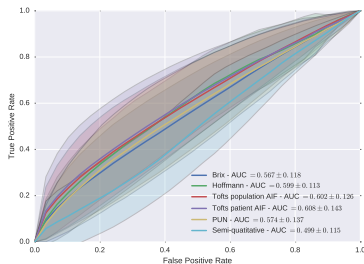


(d) Linear - AUC: 98.09

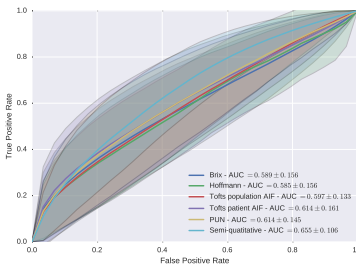


(e) SRSF - AUC: 98.30

## Quantitative and semi-quantitative models

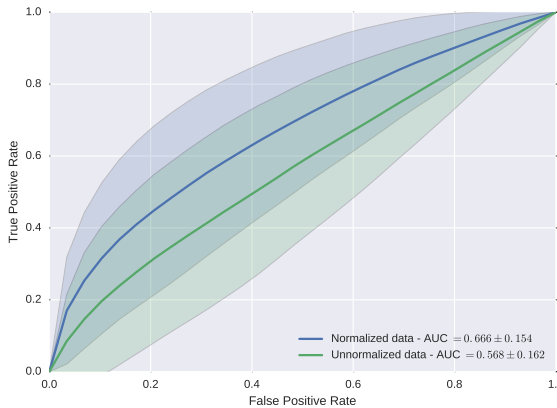


(a) Without normalization

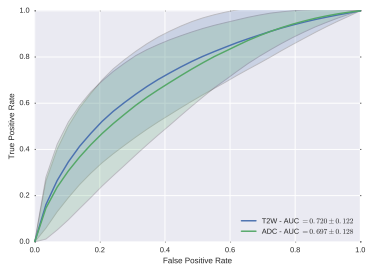
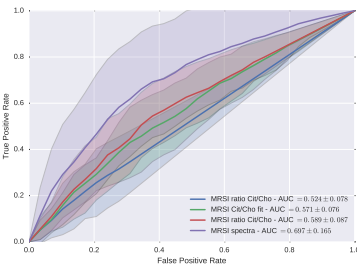


(b) With normalization

## Entire signal



## ROC analysis

(a) T<sub>2</sub>W-MRI and ADC

(b) MRSI



## Discussions

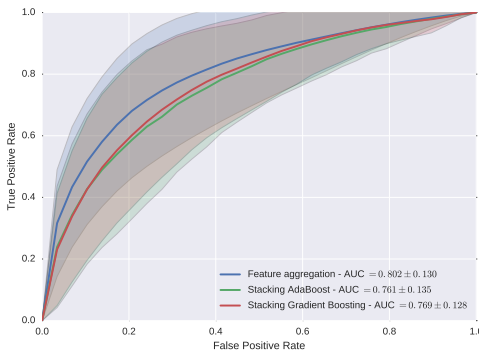
- ▶ DCE-MRI: normalized data → best performance
- ▶ DCE-MRI: entire signal better than models
- ▶ MRSI: fitting better than bounds approach
- ▶ MRSI: entire spectra better than others
- ▶ T<sub>2</sub>W-MRI < ADC = MRSI < DCE
- ▶ Performance at an “acceptable” level of discrimination - AUC ∈ [0.7, 0.8]

## Conclusions

- ✓ DCE-MRI: Use the normalized enhanced signal
- ✓ MRSI: Use the entire spectra

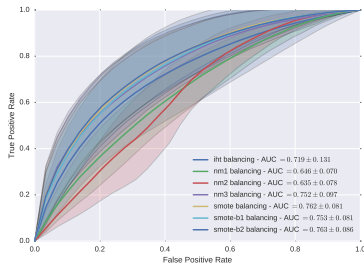
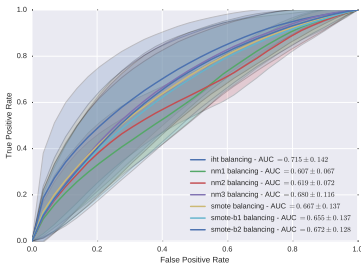
# Coarse combination

## Aggregation vs. stacking



## Conclusions

- ▶ Aggregation leads to best performance
- ✓ Gradient boosting is preferable to adaboost

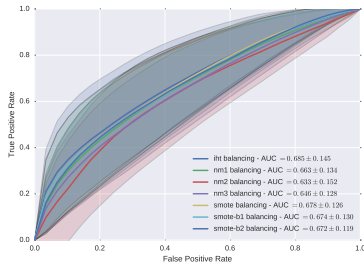
T<sub>2</sub>W-MRI and ADC(a) T<sub>2</sub>W-MRI

(b) ADC

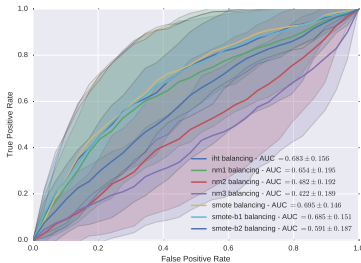
## Conclusions

- ✓ IHT → ADC
- ✓ SMOTE → T<sub>2</sub>W-MRI

## DCE-MRI and MRSI



(c) DCE-MRI



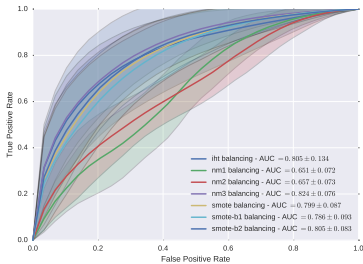
(d) MRSI

## Conclusions

- ✓ IHT → ADC and DCE-MRI
- ✓ SMOTE → T<sub>2</sub>W-MRI and MRSI

# Data balancing

## Aggregation



## Conclusions

- ✓ IHT → ADC and DCE-MRI
- ✓ SMOTE → T<sub>2</sub>W-MRI and MRSI
- ✓ NM3 → aggregate feature

T<sub>2</sub>W-MRI

Methods	Percentiles						
	15	17.5	20	22.5	25	27.5	30
ANOVA F-score	0.755 ± 0.049	0.770 ± 0.058	0.777 ± 0.064	0.782 ± 0.066	<b>0.784 ±</b> <b>0.067</b>	0.783 ± 0.072	0.782 ± 0.070

Methods	Percentiles						
	1	2	5	10	15	20	30
Gini importance	0.726 ± 0.064	0.731 ± 0.055	0.751 ± 0.065	0.758 ± 0.076	0.752 ± 0.087	0.761 ± 0.077	<b>0.764 ±</b> <b>0.079</b>

## ADC

Methods	Percentiles						
	10	12.5	15	17.5	20	22.5	25
ANOVA F-score	0.684 ± 0.123	0.713 ± 0.125	0.712 ± 0.134	0.710 ± 0.144	<b>0.714 ±</b> <b>0.142</b>	0.708 ± 0.150	0.708 ± 0.150

Methods	Percentiles						
	1	2	5	10	15	20	30
Gini importance	0.672 ± 0.132	0.690 ± 0.138	<b>0.743 ±</b> <b>0.139</b>	0.730 ± 0.136	0.730 ± 0.142	0.724 ± 0.141	0.722 ± 0.142

## DCE-MRI

Methods	Number of components or sparsity level						
	2	4	8	16	24	32	36
PCA	0.656 ± 0.133	0.634 ± 0.121	0.668 ± 0.149	0.680 ± 0.145	0.682 ± 0.146	0.679 ± 0.151	0.683 ± 0.149
Sparse-PCA	0.578 ± 0.117	0.546 ± 0.121	0.554 ± 0.097	—	—	—	—
ICA	0.657 ± 0.132	0.629 ± 0.117	0.671 ± 0.157	0.686 ± 0.158	0.691 ± 0.158	0.681 ± 0.161	0.679 ± 0.166

MRSI

Methods	Number of components or sparsity level						
	2	4	8	16	24	32	36
PCA	0.566 ± 0.120	0.575 ± 0.141	0.648 ± 0.162	0.662 ± 0.177	0.659 ± 0.184	0.671 ± 0.179	0.672 ± 0.182
Sparse-PCA	0.502 ± 0.050	0.571 ± 0.158	0.585 ± 0.111	—	—	—	—
ICA	0.567 ± 0.119	0.578 ± 0.140	0.654 ± 0.145	0.656 ± 0.167	0.650 ± 0.187	0.663 ± 0.174	<b>0.677 ± 0.171</b>

## Aggregation

Methods	Percentiles						
	10	12.5	15	17.5	20	22.5	25
ANOVA F-score	0.764 ± 0.095	0.765 ± 0.079	0.800 ± 0.083	0.817 ± 0.089	<b>0.828 ± 0.084</b>	0.822 ± 0.0084	0.815 ± 0.086

Methods	Percentiles						
	10	12.5	15	17.5	20	22.5	25
Gini importance	0.834 ± 0.085	0.834 ± 0.088	0.834 ± 0.084	<b>0.836 ± 0.083</b>	0.834 ± 0.079	0.828 ± 0.086	0.830 ± 0.077

## Conclusions

- ✓ T<sub>2</sub>W-MRI: ANOVA-based selection with 25 % of the data
- ✓ ADC: Gini importance-based selection with 5 % of the data
- ✓ DCE-MRI: ICA with 24 components
- ✓ MRSI: ICA with 36 components
- ✓ Aggregation: Gini importance with 17.5 % of the data

# Features selection/extraction

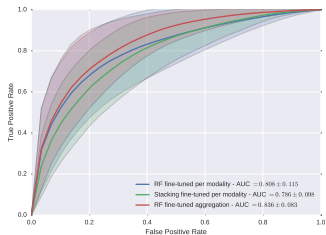
## Selected features in T<sub>2</sub>W-MRI and ADC

T <sub>2</sub> W-MRI	ADC
8 edges	1 DCT
155 Gabor filters	32 Gabor filters
2 Haralick features	1 phase congruency
1 intensity	
4 LBP	
2 phase congruency	
<hr/>	
172 features	34 features
<hr/>	

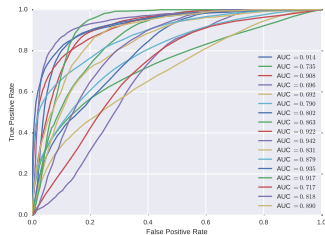
## Selected features with aggregation

T <sub>2</sub> W-MRI	ADC	DCE-MRI	MRSI		
113 Gabor filters	53 Gabor filters	14 samples	78 samples		
1 phase congruency	2 phase congruency				
4 edges					
1 intensity					
<hr/>		<hr/>			
267 features					
<hr/>					

## Aggregation vs. stacking

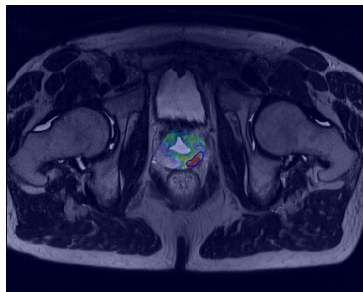


## ROC for each patient

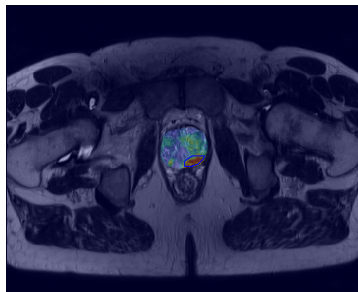


## Fine-tuned combination

“Outstanding” discrimination level



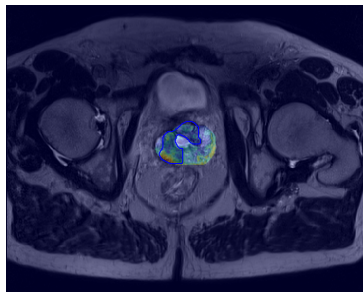
(e) AUC = 0.922



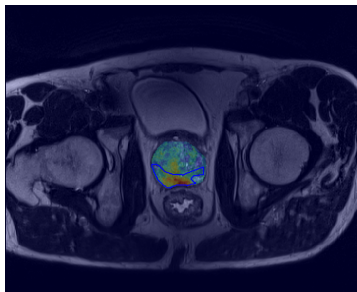
(f) AUC = 0.914

## Fine-tuned combination

“Acceptable” discrimination level



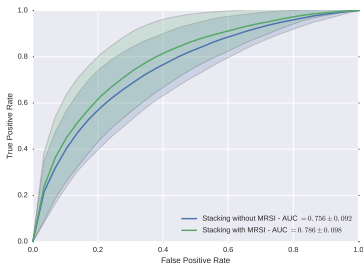
(g) AUC = 0.692



(h) AUC = 0.735

## MRSI benefit

## Stacking with/without MRSI



## MRSI in aggregation

- ✓ Features from MRSI are the most selected features

## 1 Introduction

## 2 State-of-the-art

## 3 I2CVB

## 4 Toward a mp-MRI CAD for CaP

## 5 Experiments

## 6 Conclusions

Contributions & future works

Timeline

## Research objectives

- ▶ Collect a mp-MRI dataset
- ▶ Design a CAD for CaP using all mp-MRI modalities
- ▶ Investigate normalization, feature selection/extraction, data balancing
- ▶ Implement 3D features
- ▶ Release source code and dataset

## Contributions

- ✓ Collect a mp-MRI dataset
- ✓ Design a CAD for CaP using all mp-MRI modalities
- ✓ Investigate normalization, feature selection/extraction, data balancing
- ✓ Implement 3D features
- ✓ Release source code and dataset

## Avenue for future research

- ✗ Incorporate spatial information in classification using super-voxels
- ✗ Dissociate classifiers for the PZ and CG regions
- ✗ Explore the *radiomics* features from PI-RADS v.2
- ✗ Investigate the benefit of deep-learning



# Timeline

